Mott scattering in the presence of a linearly polarized laser field

S.-M. Li
Open Laboratory of Bond Selective Chemistry, Department of Modern Physics, University of Science and Technology of China, P. O. Box 4, Hefei, Anhui 230027, People's Republic of China and Max-Planck Institut für Mikrostrukturphysik, Weinberg 2, 06120 Halle, Germany

J. Berakdar*
Max-Planck Institut für Mikrostrukturphysik, Weinberg 2, 06120 Halle, Germany

J. Chen
China Center of Advanced Science and Technology (World Laboratory), P. O. Box 8730, Beijing 100080, People's Republic of China and Department of Modern Physics, University of Science and Technology of China, P. O. Box 4, Hefei, Anhui 230027, People's Republic of China

Z.-F. Zhou
Department of Modern Physics, University of Science and Technology of China, P. O. Box 4, Hefei, Anhui 230027, People's Republic of China

(Received 4 February 2003; published 26 June 2003)

The Mott scattering in the presence of a linearly polarized laser field is investigated in the first Born approximation. The theoretical results indicate that at medium and large scattering angles, a large amount of multiphoton processes take place in the course of scattering. The photoabsorption (inverse bremsstrahlung) predominates the photoemission (bremsstrahlung). The sum rule for the multiphoton cross sections is notably violated. When the laser polarization deviates from the incident direction, the laser-modified (summed) cross section shows a considerable dependence on the azimuthal angle of the scattered electron. The dependencies of the cross section on the field strength, the frequency, the polarization direction, and the electron-impact energy are studied.

DOI: 10.1103/PhysRevA.67.063409 PACS number(s): 34.50.Rk, 34.80.Qb

I. INTRODUCTION

The physics of laser-assisted scattering of electrons by ions or atoms is well developed and documented in the literature. An overview on this field can be found in the books of Mittleman [1] and Fedorov [2] and some recent reviews [3–5]. Most of the studies have been carried out in the regime of nonrelativistic collisions and for low- or moderate-field intensities. In the presence of ultrastrong lasers, a relativistic treatment becomes imperative (even for slow electrons). This is because the averaged quiver energy acquired by a classical electron scales as the modulus square of the field strength $\mathcal{E}_0$. For contemporary laser sources having intensities in the range of 10^{18} W cm^{-2}, the averaged quiver energy may well exceed c^2 [6]. Therefore, several studies have been carried out to investigate theoretically the relativistic potential scattering assisted by an extremely intense laser field: In the treatments of Refs. [7–9], effects related to the electron spin have been neglected and the electron has been considered as a Klein-Gordon particle. Based on the theory of Refs. [10,11], Szymanowski *et al.* [12,13] investigated the spin effect in the relativistic potential scattering in the presence of a circularly polarized field, however, as they stated, the resulting expression for circularly polarized field turned out to be more tractable than for the general case of elliptical or linear polarizations. Therefore, the linearly-polarized case was not investigated in Refs. [12,13]. Panek *et al.* [14] extended the treatment to the scattering by an atomic target by modeling the atomic scattering potential as a screened Coulomb potential with a nuclear charge $Z=1$ a.u. and a screening length $\ell=1$ a.u. Hovhannisyan *et al.* [15] studied the scattering at small angles in the eikonal approximation for $Z=1$ a.u. and $\ell=4$ a.u. It should be noted, however, that for the field intensities considered in these studies (10^{16}–10^{18} W cm^{-2}), the target atom becomes extremely unstable, and will be ionized quickly by the laser field before the collision takes place.

In the present contribution, we investigate the relativistic scattering of an electron by a Coulomb potential (the Mott scattering) in the presence of a linearly polarized laser field of a medium intensity. A compact expression for the spin-unpolarized cross section is derived by the trace procedure without introducing additional quantities as have been done in previous derivations. The numerical calculation is carried out for the evaluation of the partial differential cross sections for multiphoton processes and for the cross section summed over all these processes. The cross-section dependencies on the field intensity, the frequency, the polarization direction, and on the electron-impact energy are reported.

The paper is organized as follows. In Sec. II, we set up the theory in the first Born approximation. In Sec. III, we present the numerical results for laser-modified cross sections and discuss their dependencies on the relevant parameters. Sum-

*Electronic address: jber@mpi-halle.de

mary and conclusions are given in Sec. IV. Throughout this work we use atomic units $\hbar=m=e=1$ and the Minkowski metric tensor $g_{\mu\nu}=\mathrm{diag}(1,-1,-1,-1)$.

II. THEORY

In the regime of field intensity as considered in this study, the electromagnetic field can be treated classically. For simplicity we consider a monochromatic, linearly polarized electromagnetic field described by the four-potential

$$a(x)=A\cos(kx), \tag{1}$$

where $A=(0,\mathbf{A})$, and $\mathbf{A}$ is the amplitude of the vector potential of the field. The four wave vector of the field is $k=(\omega/c,\mathbf{k})$, where ω and $\mathbf{k}$ being the frequency and the wave number, respectively. The relativistic, asymptotic electron state in the laser field, characterized by its four-momentum p, can be obtained in the explicit form upon the solution of the Dirac equation. Such a solution is called the Volkov wave function [12,16]. When normalized in volume V, it reads

$$\psi_p(x)=\left[1+\frac{\not{k}\not{A}}{2c(k\cdot p)}\right]\frac{u}{\sqrt{2QV}}\exp\left[-iq\cdot x-i\frac{p\cdot A}{c(k\cdot p)}\sin(k\cdot x)\right], \tag{2}$$

where u represents a bispinor for the free electron (satisfying the first-order Dirac equation without field). It is normalized as $\bar{u}u=u^{\dagger}\gamma^0u=2c^2$. Furthermore, we used in Eq. (2) the Feynman slash notation, i.e., for a certain four-vector v we write $\not{v}=v\cdot\gamma=g_{\mu\nu}v^{\mu}\gamma^{\nu}$. The four-vector $q=(Q/c,\mathbf{q})$ is the averaged four-momentum of the electron in the presence of the laser field, with

$$q^{\mu}=p^{\mu}-\frac{\overline{A^2}}{2c^2(k\cdot p)}k^{\mu}, \tag{3}$$

where $\overline{A^2}=A^2/2=-|\mathbf{A}|^2/2$ is the time-averaged square of the four-potential.

The scattering of the Volkov electron from the Coulomb potential

$$A^{Coul}=\left(-\frac{Z}{|\mathbf{x}|},0,0,0\right) \tag{4}$$

of the target nucleus can be described within the first Born approximation. A measure for the probability for the electron's initial state ψ_p to go over into the final state $\psi_{p'}$ is provided by the scattering matrix elements

$$S_{fi}=i\frac{Z}{c}\int d^4x\,\bar{\psi}_{p'}(x)\frac{\gamma_0}{|\mathbf{x}|}\psi_p(x). \tag{5}$$

Using the identities for Bessel functions [17],

$$e^{iy\sin u}=\sum_{l=-\infty}^{\infty}J_l(y)e^{ilu}, \tag{6}$$

$$J_{l-1}(y)+J_{l+1}(y)=\frac{2l}{y}J_l(y), \tag{7}$$

the S-matrix of Eq. (5) is recast in the form

$$S_{fi}=iZ\sum_{l=-\infty}^{\infty}\left\{\frac{1}{\sqrt{4QQ'V^2}}\frac{4\pi}{|\mathbf{q}'-\mathbf{q}+l\mathbf{k}|^2}\bar{u}'fu\times 2\pi\delta(Q'-Q+l\omega)\right\}, \tag{8}$$

where

$$f=\Delta_0\gamma_0+\Delta_1\gamma_0\not{k}\not{A}+\Delta_2\not{A}\not{k}\gamma_0+\Delta_3\not{A}\not{k}\gamma_0\not{k}\not{A}. \tag{9}$$

Here, we have introduced the following abbreviations:

$$\Delta_0=J_l(D), \tag{10}$$

$$\Delta_1=\frac{lJ_l(D)}{2c(k\cdot p)D}, \tag{11}$$

$$\Delta_2=\frac{lJ_l(D)}{2c(k\cdot p')D}, \tag{12}$$

$$\Delta_3=\frac{J_{l-2}(D)+2J_l(D)+J_{l+2}(D)}{16c^2(k\cdot p)(k\cdot p')D}, \tag{13}$$

with

$$D=\frac{p'\cdot A}{c(k\cdot p')}-\frac{p\cdot A}{c(k\cdot p)}=\boldsymbol{\mathcal{E}}_0\cdot\left[\frac{\mathbf{p}}{\omega(k\cdot p)}-\frac{\mathbf{p}'}{\omega(k\cdot p')}\right], \tag{14}$$

in which $\boldsymbol{\mathcal{E}}_0=(\omega/c)\mathbf{A}$ is the amplitude of electric field strength of the field. The cross section for the laser-assisted free-free transition is

$$d\sigma=\frac{|S_{fi}|^2}{T}\left(\frac{Vd^3q'}{8\pi^3}\right)\frac{QV}{c^2|\mathbf{q}|}=\frac{Z^2}{c^4}\sum_{l=-\infty}^{\infty}\left\{\frac{1}{|\mathbf{q}'-\mathbf{q}+l\mathbf{k}|^4}|\bar{u}'fu|^2\delta(Q'-Q+l\omega)\frac{|\mathbf{q}'|}{|\mathbf{q}|}dQ'd\Omega\right\}. \tag{15}$$

Integrating over the final-state energy Q', we obtain the cross section differentiated with the scattering solid angle Ω,

$$d\sigma=\frac{Z^2}{c^4}\sum_{l=-\infty}^{\infty}\frac{|\mathbf{q}'|}{|\mathbf{q}|}\frac{1}{|\mathbf{q}'-\mathbf{q}+l\mathbf{k}|^4}|\bar{u}'fu|^2d\Omega. \tag{16}$$

This expression can, in principle, be applied to calculate the scattering of an electron from the initial spin-polarization state s to the final spin state s'. However, in most experiments neither the initial nor the final spin states are mea-

sured. The cross section which is actually measured is obtained upon summation of Eq. (16) over the final spin states s' and then averaging over the initial spin polarizations s, i.e.,

$$d\bar{\sigma}=\frac{1}{2}\sum_{ss'} d\sigma. \tag{17}$$

The sums in this equation can be performed with the help of the standard trace procedure

$$\sum_{ss'} |\overline{u'}fu|^2=\mathrm{Tr}[f(\not{p}c+c^2)\gamma^0 f^\dagger \gamma^0(\not{p}'c+c^2)]. \tag{18}$$

Introducing the four-vector $U=(1,0,0,0)$ and using the formula [18]

$$\begin{aligned}\mathrm{Tr}(\not{v}_1\not{v}_2\cdots\not{v}_n)=&v_1\cdot v_2\mathrm{Tr}(\not{v}_3\not{v}_4\cdots\not{v}_n)\\&-v_1\cdot v_3\mathrm{Tr}(\not{v}_2\not{v}_4\cdots\not{v}_n)+\cdots\\&+v_1\cdot v_n\mathrm{Tr}(\not{v}_2\not{v}_4\cdots\not{v}_{n-1})\end{aligned} \tag{19}$$

for trace calculation successively, we conclude that the cross section has the form

$$\frac{d\bar{\sigma}}{d\Omega}=\sum_{l=-\infty}^{\infty}\frac{d\bar{\sigma}_l}{d\Omega}=\sum_{l=-\infty}^{\infty}\frac{2Z^2}{c^2}\frac{|\mathbf{q}'|}{|\mathbf{q}|}\frac{1}{|\mathbf{q}'-\mathbf{q}+l\mathbf{k}|^4}M. \tag{20}$$

The explicit form of the function M reads

$$\begin{aligned}M=&\tfrac{1}{4}\mathrm{Tr}[f(\not{p}+c)\gamma_0 f^\dagger\gamma_0(\not{p}'+c)]\\=&\tfrac{1}{4}\mathrm{Tr}[(\Delta_0\not{U}+\Delta_1\not{U}\not{k}\not{A}+\Delta_2\not{A}\not{k}\not{U}+\Delta_3\not{A}\not{k}\not{U}\not{k}\not{A})(\not{p}+c)(\Delta_0\not{U}+\Delta_1\not{A}\not{k}\not{U}+\Delta_2\not{U}\not{k}\not{A}+\Delta_3\not{A}\not{k}\not{U}\not{k}\not{A})(\not{p}'+c)]\\=&c^2[\Delta_0^2+4(\Delta_1\Delta_2-\Delta_0\Delta_3)A^2k_0^2]+\Delta_0^2(2p_0p_0'-p\cdot p')+\Delta_1^2\{2A^2[(k\cdot p)(k\cdot p')-2k_0p_0'(k\cdot p)]\}+\Delta_2^2\{2A^2[(k\cdot p)(k\cdot p')\\&-2k_0p_0(k\cdot p')]\}+\Delta_3^2[8A^4k_0^2(k\cdot p)(k\cdot p')]+2\Delta_0\Delta_1[2k_0p_0'(A\cdot p)+(k\cdot p)(A\cdot p')-(k\cdot p')(A\cdot p)]\\&+2\Delta_0\Delta_2[2k_0p_0(A\cdot p')+(k\cdot p')(A\cdot p)-(k\cdot p)(A\cdot p')]+2\Delta_0\Delta_3\{2A^2k_0[k_0(p\cdot p')-p_0(k\cdot p')-p_0'(k\cdot p)]\}\\&+2\Delta_1\Delta_2\{4k_0^2(A\cdot p)(A\cdot p')+2A^2[k_0p_0(k\cdot p')+k_0p_0'(k\cdot p)-k_0^2(p\cdot p')-(k\cdot p)(k\cdot p')]\}+2\Delta_1\Delta_3[-4A^2k_0^2(k\cdot p)\\&\times(A\cdot p')]+2\Delta_2\Delta_3[-4A^2k_0^2(k\cdot p')(A\cdot p)].\end{aligned} \tag{21}$$

III. RESULTS AND DISCUSSION

In this section, we present and discuss the numerical results for cross sections of the Mott scattering assisted by a linearly polarized laser field. The target is assumed to be an infinitely massive nucleus having a charge $Z=10$. The origin of the coordinate system is chosen to be on the target. The z axis is set along the incident electron momentum $\mathbf{p}$, the y axis along the direction of the field wave vector $\mathbf{k}$, and the electric-field vector $\boldsymbol{\mathcal{E}}_0$ of the field lies in the xz plane.

Figure 1 displays the partial differential cross sections $d\bar{\sigma}_l/d\Omega$ versus the net photon number l transferred between the colliding system and the laser field. The electron-impact energy is $T_i=mc^2=0.511$ MeV (the corresponding Lorentz factor $\gamma_L=Q/mc^2=(T_i+mc^2)/mc^2=2$), field strength is $\mathcal{E}_0=0.01$ a.u.$=5.14\times10^7$ V cm^{-1}, and photon energy (field frequency) is $\hbar\omega=1.17$ eV. The laser polarization is chosen to be parallel to the incident momentum. At a small scattering angle [$\theta=1°$ in Fig. 1(a)], only a few multiphoton processes are important, and the partial differential cross section $d\bar{\sigma}_l/d\Omega$ is sharply peaked around $l=0$. At large scattering angles [$\theta=90°$ in Fig. 1(b) and 180° in Fig. 1(c)], a large amount of multiphoton processes have significant contributions, the origin of this behavior will be given below. The magnitudes for $d\bar{\sigma}_l/d\Omega$ varies in the range of few orders for different l. Furthermore, the contributions of various l-photon processes are cut off at two edges which are asymmetric with respect to $l=0$. The cutoff for positive l is a consequence of the energy conservation imposed on Eq. (15). On the other hand, the origin of the cutoff for negative values of l can be inferred by the properties of the Bessel function $J_l(D)$ when its argument D is approximately equal to its order l. This has already been pointed out in Ref. [12]. The results shown in Fig. 1(b,c) indicate that photon absorption processes (i.e., $l<0$ contributions) predominant the photon emission ones ($l>0$).

Figure 2 shows the differential cross sections summed over all multiphoton processes, as given by Eq. (20). Included in Fig. 2 are the results for the laser-free scattering (solid line) and for the laser-assisted scattering (dashed line for $\boldsymbol{\mathcal{E}}_0\|\mathbf{p}$, and dotted line for $\boldsymbol{\mathcal{E}}_0\perp\mathbf{p}$). At small angles, the summed cross section is almost unmodified by laser. Classically the small scattering angle region corresponds to large impact parameters, for which the orbits of the incoming electron are hardly deflected by the target Coulomb field. As it is known, a free-electron exchange energy with the radiation field only in the presence of a charged scattering center (the atomic nucleus in the present case). The weaker the target interaction is, the lesser is the ability of the electron to exchange photons with the radiation field. Thus, for medium-

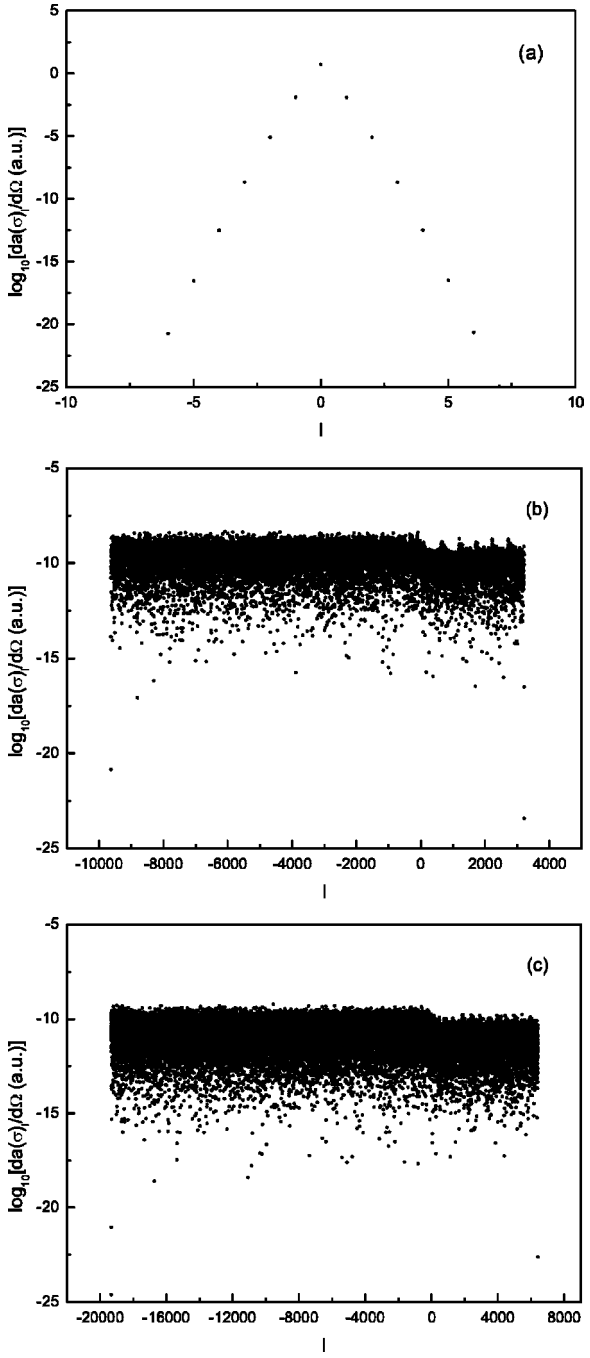

FIG. 1. The multiphoton cross sections for the laser-assisted Mott scattering at an electron-impact energy of $T_i = mc^2 = 0.511$ MeV as a function of the number of the involved photons l. The scattering angles are in (a) $\theta = 1°$, in (b) $\theta = 90°$, and in (c) $\theta = 180°$. The laser field is linearly polarized along the incident direction of the electron. The field strength is $\mathcal{E}_0 = 0.01$ a.u. $= 5.14 \times 10^7$ V cm^{-1}, and the photon energy (field frequency) $\hbar\omega = 1.17$ eV.

field intensities as considered here, the laser-induced modifications of the cross section at small angles are negligible. In contrast, for medium and large scattering angles the momentum transfer during the collision is large, i.e., the electrons are strongly scattered from the Coulomb field of the target nucleus. The strong coupling of the electron to the ion allows

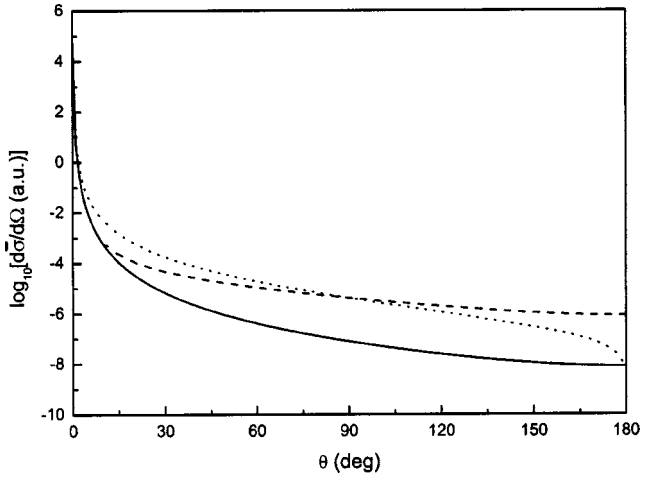

FIG. 2. The differential cross sections summed over all the multiphoton processes. The solid line is the result for the laser-free case, whereas the dashed line is the result for the laser-modified cross section for the geometry $\boldsymbol{\mathcal{E}}_0 \| \mathbf{p}$. The dotted line stands for the laser-modified cross section for the case $\boldsymbol{\mathcal{E}}_0 \perp \mathbf{p}$ (the azimuthal angle is $\phi = 0°$). The impact energy and the laser parameters are the same as in Fig. 1.

an efficient exchange of a large number of photons with the laser field. Therefore, the summed cross section is greatly enhanced at large scattering angles [also cf. Figs. 1(a–c)].

In the backward direction ($\theta = 180°$), the modification of the cross section by the laser field in the geometry $\boldsymbol{\mathcal{E}}_0 \| \mathbf{p}$ is of most significant. In contrast, if we choose $\boldsymbol{\mathcal{E}}_0 \perp \mathbf{p}$, the laser-assisted cross section at $\theta = 180°$ drops to the results for laser-free case. This behavior is due to the properties of the Bessel functions in Eqs. (10)–(13). When the electric-field polarization is parallel to the incident direction, their argument D [see Eq. (14)] reaches a maximum and hence many partial cross sections contribute to the summed cross section. On the other hand, for the perpendicular geometry we find $D = 0$. Therefore, we obtain the same result for the cross section in the presence of the laser as that for the laser-free.

Figure 3 indicates that at the polar scattering angle $\theta = 90°$, the summed differential cross section is strongly dependent on the azimuthal angle ϕ of the scattered electron. In contrast to the case of the nonrelativistic scattering in which the cross section is symmetric about $\phi = 180°$, the cross sections for relativistic collisions do not show such a symmetry property. This asymmetry is inferred from the asymmetric properties of the factor $p' \cdot k$ that occurs in the denominator in the argument D of Eq. (14) [which in turn enters the Bessel functions appearing in Eqs. (10)–(13)]. At $\phi = 90°$ and 270°, the cross section in the presence of the laser drops to the results for the laser-free case, because at these angles the argument D of the Bessel functions occurring in Eqs. (10)–(13) vanishes.

Figure 4 reveals the dependence of the summed cross section on the laser field strength. The field strength enters the determining equations for the cross section through the argument D of the Bessel functions in Eqs. (10)–(13), and through the A-dependent terms in Eq. (21). Although for each multiphoton process, the Bessel functions in the partial cross section oscillate with the field strength, the summed

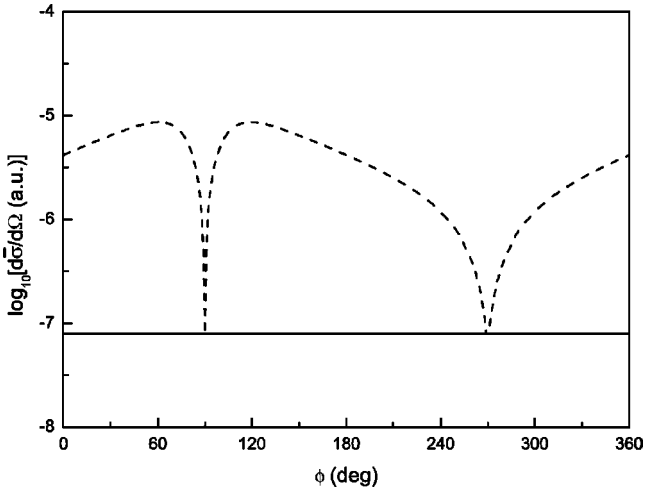

FIG. 3. The azimuthal-angle dependence of the summed differential cross section for the geometry $\boldsymbol{\mathcal{E}}_0 \perp \mathbf{p}$ at the scattering angle $\theta = 90°$. The solid line represents the result for the laser-free cross section. The dotted line is the result for the cross section when the laser is present. The impact energy and the laser parameters are the same as in Fig. 1.

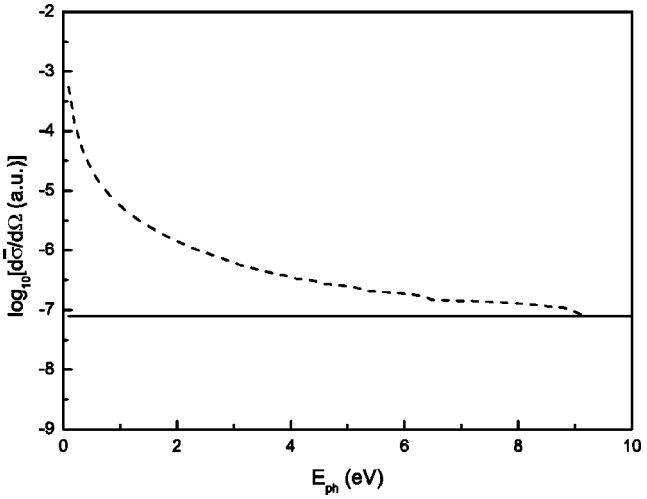

FIG. 5. The photon energy (field frequency) dependence of the summed differential cross section for the field strength $\mathcal{E}_0 = 5.14 \times 10^7$ V cm^{-1} at $\theta = 90°$ and $\phi = 0°$. The solid line shows the cross section for the laser-free case. The dashed line is the result for the cross section when the laser is present. The impact energy and the laser polarization geometry are the same as in Fig. 1.

cross section increases steadily by about two orders as the field strength increases from 0 to 10^8 V cm^{-1}. The stronger the field is, the more the electron state is distorted, thus the more the cross section is modified.

In Fig. 5, the frequency (photon energy) dependence of cross section is depicted. Contrary to the field strength dependence, the lower the frequency is, the more the summed cross section is modified. As the photon energy increases to about 9 eV, both cross sections for the laser-assisted and for the laser-free cases merge together. From a mathematical point of view, this behavior is comprehensible because according to Eq. (14), when the field strength $\mathcal{E}_0$ is fixed, the argument D of Bessel functions is inversely proportional to ω^2 through k and A. In addition to the Bessel-function-determined factors Δ_0, Δ_1, Δ_2, and Δ_3, Eq. (21) also contains other factors that depend on k and A. In these factors however, the ω dependence is canceled. Physically, the decline of the laser-assisted cross section with increasing laser frequencies is due to the inertia of the electron in responding to the laser-field oscillations. In Fig. 5 we also observe some smooth steps in the cross section, which are caused by the oscillations of the Bessel functions.

Figure 6 gives the dependence of the summed cross section on the (linear) polarization direction of the field. The

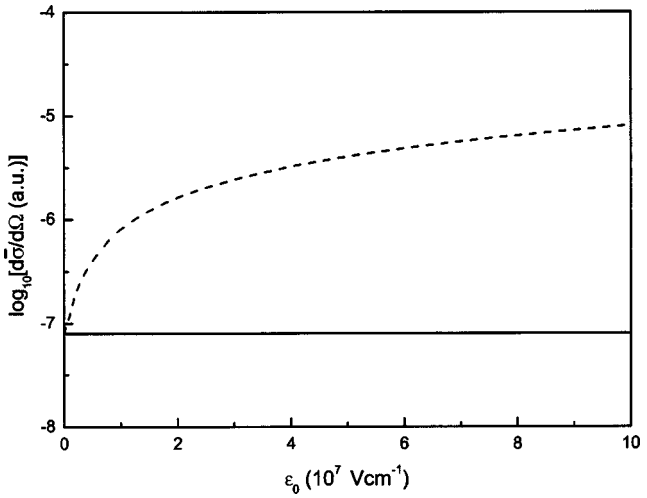

FIG. 4. The field strength dependence of the summed differential cross section at $\theta = 90°$ and $\phi = 0°$ for the field frequency $\hbar\omega = 1.17$ eV. The solid line is the result for the laser-free cross section, whereas the dashed line stands for the laser-assisted cross section. The impact energy and the laser polarization geometry are the same as in Fig. 1.

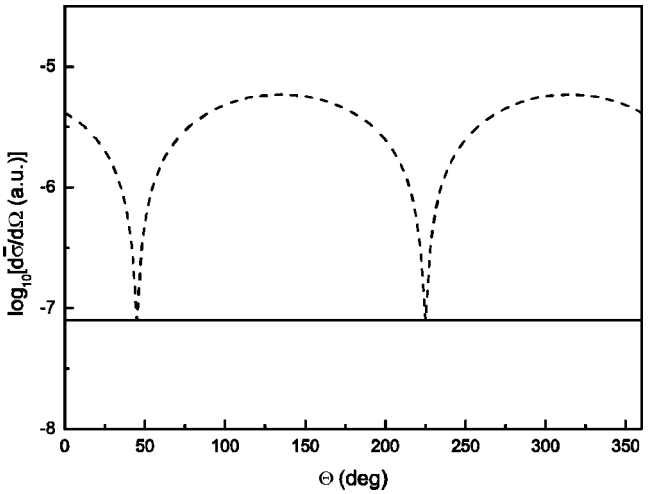

FIG. 6. The summed differential cross sections versus the polar angle of the polarization vector of the field (the polarization vector $\boldsymbol{\mathcal{E}}_0$ varies in the zx plane) for $\theta = 90°$ and $\phi = 0°$. The solid line shows the cross section for the laser-free case, whereas the dashed line stands for the cross section in the presence of the laser. The impact energy and the laser parameters are the same as in Fig. 1.

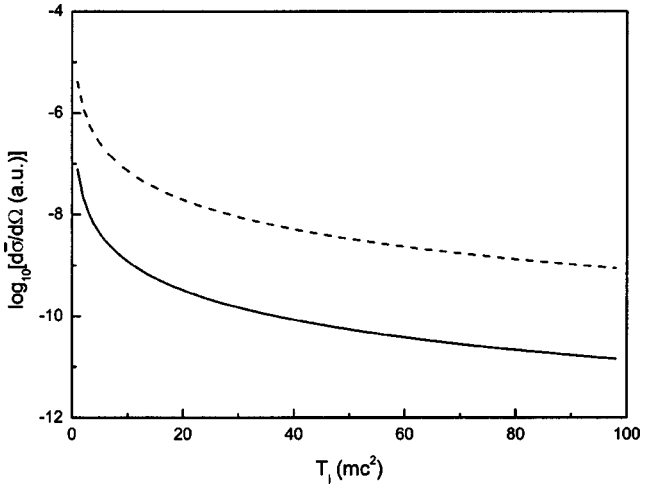

FIG. 7. The summed differential cross section at $\theta=90°$ and $\phi=0°$ versus the kinetic energy of the incident electron. The solid line displays the Mott-scattering cross section for the laser-free case, whereas the dashed line indicates the laser-modified result. The laser parameters and the polarization geometry are the same as in Fig. 1.

polarization dependence is approximately periodic. This is explained by the periodic nature of the argument D [Eq. (14)] of the Bessel functions. When the magnitudes of the field strength and the momenta of the electron in the initial and the final states are fixed, the scalar product between $\boldsymbol{\mathcal{E}}_0$ and $\mathbf{p}$ (or $\mathbf{p}'$) varies periodically with the polar angle Θ of $\boldsymbol{\mathcal{E}}_0$.

Figure 7 shows the summed differential cross section versus the kinetic energy of the incident electron at the scattering angle $\theta=90°$. In the energy regime considered here, the free-free transition cross section is enhanced by more than one order of magnitude, this is attributed to the large amount of multiphoton processes accompanying the scattering.

IV. CONCLUSIONS

The general features of the Mott scattering are modified decisively when a radiation field is present. The colliding system can exchange a large amount of photons with the laser field, depending on the properties of the field and on the Mott-scattering geometry. Although in this work we studied such processes in the simple case of linearly polarized laser field in geometries different from previous investigations [12–15], the treatment can be readily extended to the case of a general polarization of the field and to the scattering by atomic targets.

The theoretical results for the linear polarization case show that the Mott cross section is greatly enhanced by the presence of the laser field within a wide energy range of impact electron. The laser-induced inverse bremsstrahlung dominates the induced bremsstrahlung. The stronger the laser and the lower the frequency are, the more prominent the cross section enhancement will be.

ACKNOWLEDGMENTS

This work was supported by the National Natural Science Foundation of China under Grant Nos. 10074060 and 10075043. S.-M.L. would like to thank the DAAD for the financial support of his stay at the MPI in Halle, Germany.

[1] M.H. Mittleman, *Introduction to the Theory of Laser-Atom Interactions* (Plenum, New York, 1993).
[2] M.V. Fedorov, *Atomic and Free Electrons in a Strong Light Field* (World Scientific, Singapore, 1997).
[3] P. Francken and C.J. Joachain, J. Opt. Soc. Am. B **7**, 554 (1990).
[4] F. Ehlotzky, A. Jaroń, and J.Z. Kamiński, Phys. Rep. **297**, 63 (1998).
[5] F. Ehlotzky, Phys. Rep. **345**, 175 (2001).
[6] H.M. Milchberg and R.R. Freeman, J. Opt. Soc. Am. B **13**, 51 (1996).
[7] F. Ehlotzky, Opt. Commun. **66**, 265 (1988).
[8] J.Z. Kamiński and F. Ehlotzky, Phys. Rev. A **59**, 2105 (1999).
[9] P. Panek, J.Z. Kamiński, and F. Ehlotzky, Can. J. Phys. **77**, 591 (1999).
[10] M.M. Denisov and M.V. Fedorov, Zh. Eksp. Teor. Fiz. **53**, 1340 (1967) [Sov. Phys. JETP **26**, 779 (1968)].
[11] S.P. Roshchupkin, Laser Phys. **3**, 414 (1993); **7**, 873 (1997); Zh. Eksp. Teor. Fiz. **106**, 102 (1994) [JETP **79**, 54 (1994)]; **109**, 337 (1996) [**82**, 177 (1996)].
[12] C. Szymanowski, V. Véniard, R. Taïeb, A. Maquet, and C.H. Keitel, Phys. Rev. A **56**, 3846 (1997).
[13] C. Szymanowski and A. Maquet, Opt. Express **2**, 262 (1998).
[14] P. Panek, J.Z. Kamiński, and F. Ehlotzky, Phys. Rev. A **65**, 033408 (2002).
[15] T.R. Hovhannisyan, A.G. Markossian, and G.F. Mkrtchian, Eur. Phys. J. D **20**, 17 (2002).
[16] V.B. Berestetskii, E.M. Lifshitz, and L.P. Pitaevskii, *Quantum Electrodynamics*, 2nd ed. (Pergamon, Oxford, 1982).
[17] I.S. Gradshteyn and I.M. Ryzhik, *Tables of Integrals, Series, and Products* (Academic, New York, 1980).
[18] W. Greiner and J. Reinhardt, *Quantum Electrodynamics*, 2nd ed. (Springer-Verlag, Berlin, 1994).